6-15-1999

Local Data Assimilation in the Estimation of Barotropic and Baroclinic Open Boundary Conditions

Igor Shulman
University of Southern Mississippi

James K. Lewis
Ocean Physics Research and Development

John G. Mayer
University of Southern Mississippi

JOURNAL OF GEOPHYSICAL RESEARCH, VOL. 104, NO. C6, PAGES 13,667-13,680, JUNE 15, 1999

Local data assimilation in the estimation of barotropic and baroclinic open boundary conditions

Igor Shulman

Institute of Marine Sciences, University of Southern Mississippi, Stennis Space Center

James K. Lewis[1]

Ocean Physics Research and Development, Long Beach, Mississippi

John G. Mayer

Department of Scientific Computing, University of Southern Mississippi, Hattiesburg

Abstract. The problem of data assimilation in the specification of open boundary conditions for limited area models is addressed in this paper. Optimization approaches are detailed, which are based on combining available data on an open boundary with the physics of the hydrodynamical model. In our case the physics is in terms of the flux of energy through the open boundary. These optimized boundary conditions, for both barotropic and baroclinic situations, interpreted physically as special linearizations of the Bernoulli equation for each normal mode. Because of the complexity of decomposing variables into normal modes for open boundaries with varying bathymetry, we present two alternative approaches. The first is a simplification of the optimized baroclinic boundary condition based on normal modes. The second makes use of empirical orthogonal functions instead of normal modes. The results of testing and comparisons of these approaches are presented for coupling coarse- and fine-resolution models. In this case our approach is in assimilating values and variables from a large-scale model (along the open boundaries of a limited area model). In the proposed coupling schemes the energy fluxes are estimated either from coarse or from fine-grid model results. With the progress of oceanographic observing systems we would like to explore ways of combining model outputs with the oceanographic measurements in order to estimate energy fluxes used in optimized open boundary conditions.

1. Introduction

The development of limited area coastal models is very important for operational predictions in coastal regions. The treatment of open boundaries is one of the most interesting problems to be solved while modeling oceanic phenomena, especially in finite coastal ocean areas. In most ocean models, open boundary conditions (OBCs) are chosen locally, i.e., depending on the solution of the governing equations near the boundary. Many approaches of the local type have been developed [*Reid and Bodine*, 1968; *Orlanski*, 1976; *Chapman*, 1985; *Blumberg and Kantha*, 1985; *Flather*, 1976].

[1]Now at Scientific Solutions, Inc., Kalaheo, Hawaii.

Paper number 1999JC900022.
0148-0227/99/1999JC900022$09.00

The results of numerical studies show successful use of many local-type boundary conditions in practical applications. However, it is known [*Oliger and Sundstrom*, 1978; *Bennett*, 1992] that the local treatment of open boundaries for primitive equation hydrostatic models is an ill-posed problem in that it is difficult to prove that a unique solution exists that is continuously dependent on boundary values. During recent years a new approach for specifying open boundary conditions for limited area ocean models has been developed. This approach starts with the work by *Bennett and McIntosh* [1982] in which data assimilation is used to estimate open boundary conditions. With this method, available data in the interior of a model are combined with model dynamics in an inverse problem to determine the open boundary conditions (in this case the local treatment of open boundary conditions is avoided). This technique was developed further by *Bennett* [1992], *Seiler* [1993], and *Zou et al.* [1993]. Other recent research on this subject has been performed by *Bogden et al.* [1996] and *Gunson* *and Malanotte-Rizolli* [1996a, b]. The inverse approach leads to a stable determination of open boundary conditions, and successful examples of its applications have been shown. Although this inverse method is certainly a viable approach, it requires a tremendous amount of computer time and memory, significant additions and changes to the hydrodynamical model's code (for example, the integration of adjoint equations), and some a priori hypotheses about the statistical properties of errors in the observations. Because of these factors, the development of less optimal but more computationally affordable data assimilation methods has been pursued for determining open boundary conditions [see, e.g., *Zou et al.*, 1995].

For barotropic conditions, *Shulman and Lewis* [1995] proposed a local data assimilation approach for specifying barotropic open boundary conditions. In this approach, values of variables on the open boundary can be determined via a specific optimization problem that provides the best fit to available observations on the open boundary and to the flux of energy through the open boundary. The optimization problem has the following physical interpretation: the boundary values are estimated by minimization of the potential energy of differences between the reference and model variables on the open boundary under the constraint of the flux of energy through the open boundary. It has been shown that the optimized versions of some well-known radiation boundary conditions [*Flather*, 1976; *Reid and Bodine,* 1968] can be derived using this approach [*Shulman and Lewis,* 1995]. The optimized versions of these barotropic radiation conditions are nonlocal boundary conditions that preserve the physics and simplicity of the numerical implementation of the original nonoptimized boundary conditions. The results of our previous work have shown that these types of optimized boundary conditions allow a model to be less sensitive to the errors in the data being specified at the open boundaries.

Here we present a second optimized formulation for barotropic boundary conditions. In this second formulation the boundary values are estimated by minimization of the kinetic energy of differences between the reference and model variables on an open boundary under the constraint of the flux of energy through the open boundary. The two barotropic methods are shown to provide the flexibility of being able to specify vertically integrated currents or sea level at an open boundary.

We also discuss the assimilation of baroclinic information on the basis of an energy flux approach. Many models use so-called splitting techniques to separate fast moving external gravity waves and slower moving internal gravity waves [see *Blumberg and Mellor*, 1987]. In such cases the separation of the vertically integrated governing equations (barotropic external mode) and the equations governing vertical structure (baroclinic internal mode) is introduced. Boundary conditions can be formulated for the barotropic and baroclinic modes separately and then adjusted to take into account the different truncation errors for those modes [*Blumberg and Mellor*, 1987]. Moreover, in the baroclinic mode the variables can be decomposed into a set of the orthogonal modes, and boundary conditions can be prescribed for each mode (*Jensen*, 1993; *O'Brien*, personal communication, 1996). In handling baroclinic boundary conditions we will follow this philosophy of splitting the barotropic and baroclinic modes. Baroclinic optimized OBCs are derived in the form of a special linearization of the Bernoulli equation for each normal mode. Because of the complexity of the decomposition of normal modes for varying bathymetry at an open boundary, two additional approaches are put forward to derive baroclinic boundary conditions. The first is a simplified modal baroclinic condition, with this simplification representing an average over all the baroclinic modes [*Shulman and Lewis,* 1996]. The second is the use of empirical orthogonal functions (EOFs) instead of normal modes. The results of testing and comparisons of these various approaches (normal mode decomposition, the simplified modal baroclinic boundary condition, and the use of empirical orthogonal functions) are presented.

Section 2 and 3 describe the theory and development of the barotropic and baroclinic optimized open boundary conditions. We then move from developmental aspects to applications in section 4. Section 4 presents the results of employing optimized baroclinic boundary conditions over an idealized shelf/shelf slope region for two different test cases. These test cases concentrate on the baroclinic boundary conditions whereas *Shulman and Lewis* [1995] considered the barotropic boundary conditions. A discussion and conclusions appear in section 5.

2. Approach

There are many different conditions that could be utilized on open boundaries. For example, we might choose estimates of energy, momentum, or mass fluxes and use these estimates in different fashions for developing open boundary conditions. In this study we follow *Shulman and Lewis* [1995] and choose energy flux as a constraint to be used in developing boundary conditions. As we will show this approach works, and the derived boundary conditions have sound physical interpretations. It should be noted that the momentum flux could be utilized, but this will result in a nonlinear constraint.

Let us consider the following function P:

$$P = p + \rho\Omega \tag{1}$$

where p is pressure, ρ is density, and Ω is potential energy per unit mass. Function P can be interpreted as a "modified" pressure [*Batchelor*, 1967, p.176], as a part of the Bernoulli function, or as the Montgomery potential multiplied by ρ. According to (1) and the hydrostatic approximation the modified pressure at depth z' (z' is positive upward) has the following representation:

$$P = \rho_r g\eta + g\Phi \qquad \Phi = -\int_{z'}^{\eta} z\frac{\partial\rho}{\partial z}\,dz \tag{2}$$

where η is the sea surface elevation, g is the gravitational constant, and ρ_r is a constant reference density. Now suppose we have some data at the open boundaries pertaining to the modified pressure and the outward normal component of velocity. These reference values will be denoted as P^o and u_n^o. From these we will develop barotropic and baroclinic conditions for open boundaries.

2.1. Barotropic Boundary Conditions

Let us introduce the following notations: H is the water depth, Γ is the open boundary, $s \in \Gamma$, and u_n is the outward normal component of the velocity on the open boundary at time t. We introduce the following numerical constraint representing the differences between the vertically averaged reference values and the vertically averaged values from a limited area model (vertically averaged values will be denoted by overbars):

$$-\int_\Gamma H(\overline{P} - \overline{P^o})(\overline{u}_n - \overline{u_n^o})\, ds = \overline{F}_t \tag{3}$$

Suppose some numerical estimate of $\overline{F}_t$ is known. In this case, $\overline{F}_t$ can be interpreted as the energy flux on the open boundary of the difference between the reference and model-predicted values of modified pressure and velocity. Consider the following optimization problem constrained by the above function $\overline{F}_t$

$$\min_{\overline{u}_n}[J = 0.5 \int_\Gamma H\rho_r(\overline{u}_n - \overline{u_n^o})^2\, ds] \tag{4}$$

In terms of physical processes the above problem means that we will choose barotropic boundary conditions that minimize the kinetic energy of the differences between the reference and model velocities on the open boundaries under the constraint of the flux of the energy. Using the Lagrangian method [*Fletcher,* 1987] to solve the optimization problem, we minimize

$$\min_{\overline{u}_n}\{J - \mu_t[\int_\Gamma H(\overline{P} - \overline{P^o})(\overline{u}_n - \overline{u_n^o})\, ds + \overline{F}_t]\}$$

where μ_t is a constant (the Lagrangian multiplier). Thus the solution of the optimization problem satisfies the following optimality condition:

$$\frac{\delta J}{\delta \overline{u}_n} - \mu_t H(\overline{P} - \overline{P^o}) = 0$$

Introducing $\lambda_t' = 1/\mu_t$ and taking into account that $\delta J/\delta\overline{u}_n = H\rho_r(\overline{u}_n - \overline{u_n^o})$, the solution has the form

$$\overline{u}_n = \overline{u_n^o} + \frac{1}{\lambda_t'}\frac{(\overline{P} - \overline{P^o})}{\rho_r} \tag{5}$$

where multiplier λ_t' has the dimension of ms^{-1} and can be determined by substituting (5) into the constraint (3). Equation (5) is the more general form of the results presented by *Shulman and Lewis* [1995]. In this case, (5) takes into consideration the impact of the density structure of the water column. If we introduce the nondimensional term $\lambda_t^o = \sqrt{gH}/\lambda_t'$ and make the Boussinesq approximation, the solution becomes the familiar

$$\overline{u}_n = \overline{u_n^o} + \lambda_t^o(g/H)^{\frac{1}{2}}(\eta - \eta^o) \tag{6}$$

which is an optimized form of the open boundary condition for the barotropic mode put forward by *Flather* [1976] and used in a number of studies. When $\overline{u_n^o} = 0$, condition (6) becomes

$$\overline{u}_n = \lambda_t^o(g/H)^{\frac{1}{2}}(\eta - \eta^o) \tag{7}$$

Note that condition (7) is the boundary condition introduced by *Reid and Bodine* [1968] but with the addition of the multiplier λ_t^o.

The above formulations provide a means of specifying velocity at an open boundary on the basis of available reference data for sea level and/or currents. However, we often are faced with the need to specify sea level at the open boundary as opposed to velocity. A scheme for specifying sea level at the open boundary can be also formulated. Instead of the optimization problem (equations (3)-(4)), the minimization of the following functional can be considered:

$$\min_{\overline{P}}[J = \frac{1}{2}\int_\Gamma (H/g)^{1/2}(\overline{P} - \overline{P^o})^2/\rho_r\, ds] \tag{8}$$

under constraint (3). The solution of the optimization problem, (3)-(8), has the structure of (5) rewritten for $\overline{P}$ as the unknown. If we neglect the density differences for the barotropic mode, we will come up with the following optimization problem instead of (3)-(8):

$$\min_{\eta}[J = \frac{g\rho_r}{2}\int_\Gamma (gH)^{1/2}(\eta - \eta^o)^2\, ds] \tag{9}$$

$$-g\rho_r \int_S H(\eta - \eta^o)(\overline{u_n} - \overline{u^o{}_n})\, ds = \overline{F_t} \tag{10}$$

Problems (9)-(10) have a physical interpretation that causes us to choose barotropic boundary conditions that minimize the potential energy (instead of kinetic energy for (3)-(4)) of the differences between the reference and model variables on open boundaries under the constraint of the flux of energy through the open boundary. For the solution we again have the optimized form of the open boundary condition introduced by *Flather* [1976] but rewritten this time with the sea surface elevation as the unknown:

$$\eta = \eta^o + \Lambda_t^o(H/g)^{\frac{1}{2}}(\overline{u}_n - \overline{u_n^o}) \tag{11}$$

In (11) we use the notation Λ_t^o for the Lagrange multiplier in order to distinguish it from the multiplier λ_t^o in (6). When $\overline{u_n^o} = 0$, the boundary condition (11) becomes the optimized version of the *Reid and Bodine* [1968] condition but rewritten with the sea surface elevation as the unknown. The choice of the optimization problem (3)-(4) or (9)-(10) and corresponding boundary conditions (6) or (11) may be based on the numerical scheme of a hydrodynamical model. In this study we use a version of the *Blumberg and Mellor* [1987] model. This model uses the staggered Arakawa C grid; sea surface elevation is calculated at the center of the grid cell, while the velocities are calculated on the sides of the grid box. If the open boundary crosses the location of the sea surface elevation (center of the grid), the boundary condition (11) can be used. In this case the η at the open boundary is calculated from (11) using the specified η^o and $\overline{u_n^o}$ (perhaps from observations) and u_n from the next interior model grid cell. Then the velocity on the open boundary is calculated using the linearized momentum equation. In the situation where the open boundary crosses the location of velocity the boundary condition (6) can be used. In this case the velocity on the open boundary is specified from (6) by using the sea surface elevation calculated from the continuity equation and located a half of a grid inside of the open boundary.

2.2. Baroclinic Boundary Conditions

2.2.1. Baroclinic modes: Modal decomposition. We now consider the decomposition of variables in the vertical along open boundaries in terms of M modes. As such, the variables are asterisked to represent values after having subtracted the vertical average (e.g., $P^* = P - \overline{P}$). We begin by representing our modified pressures as the sum of normal modes on the open boundaries:

$$P^* = \sum_{m=1}^{M} \psi_m(z)\varphi_m(x,y,t)$$

$$P^{o*} = \sum_{m=1}^{M} \psi_m(z)\varphi_m^o(x,y,t) \qquad (12)$$

where $\psi_m(z)$ are the normal modes that are orthogonal to each other in that

$$\int_{-H}^{0} \frac{1}{\rho_0}\psi_n(z)\psi_m(z)dz = 0 \qquad n \neq m$$

where $\rho_0(z)$ is the basic state of the density stratification on the open boundary. The functions φ_m and φ_m^o are the modal amplitudes and allow for the representation of the horizontal structure of the modes:

$$\varphi_m(x,y,t) = \frac{\int_{-H}^{0} \frac{1}{\rho_0} P^* \psi_m(z)dz}{\int_{-H}^{0} \frac{1}{\rho_0}\psi_m^2(z)dz} \qquad (13)$$

Following along the lines of the work for the barotropic mode, we can write the function F_t^m as

$$F_t^m = -\int_\Gamma [\int_{-H}^{0} (u_n^* - u_n^{o*})\psi_m(z)dz] \bullet [\varphi_m(s,t) - \varphi_m^o(s,t)]ds \qquad (14)$$

such that F_t^m represents the contribution of the mth mode to the energy flux on the open boundary resulting from the differences between the reference and the model-predicted values of modified pressure and velocity. Suppose we have some estimate of F_t^m. Now we choose the following optimization problem constrained by the functions F_t^m:

$$\min_{u_n^*} [J = 0.5 \int_\Gamma \int_{-H}^{0} \rho_0 (u_n^* - u_n^{o*})^2 \, dz \, ds] \qquad (15)$$

As before, we can provide a physical interpretation of this optimization problem: boundary values are chosen for the baroclinic velocity that minimizes the kinetic energy of the differences between the reference and model velocities on the open boundary under the constraints that represent the contribution of each mode to the energy flux on the open boundary. The solution to the above optimization problem provides a normal mode representation for the velocity on the open boundary and has the form

$$u_n^* = u_n^{o*} + \sum_{m=1}^{M} \frac{1}{\lambda_t^m} \frac{\psi_m(z)}{\rho_0} [\varphi_m(s,t) - \varphi_m^o(s,t)] \qquad (16)$$

$$\frac{1}{\lambda_t^m} = -F_t^m / [\int_{-H}^{0} \frac{1}{\rho_0}\psi_m^2(z)dz \bullet \int_\Gamma [\varphi_m(s,t) - \varphi_m^o(s,t)]^2 ds] \qquad (17)$$

The dimension of λ_t^m is ms^{-1}. It is shown in Appendix A that the average of λ_t^m is the group velocity of the mth mode. For the mth mode we introduce velocity $\mathbf{U}_m$ with the following normal and tangential components:

$$U_{m,n} = -\lambda_t^m \qquad U_{m,\tau} = 0$$

In this case the modal component for (16) can be rewritten in the following form:

$$\mathbf{u_m^*} \bullet \mathbf{U}_m + P_m^*/\rho_0 = \mathbf{u_m^{O*}} \bullet \mathbf{U_m} + P_m^{o*}/\rho_0$$

where $\mathbf{u_m^*}$ is velocity for the mth mode, $\mathbf{u_m^{O*}}$ is reference velocity for the mth mode, P_m^* is the mth mode of the modified pressure (see (12)), and P_m^{o*} is the mth mode of the reference modified pressure. The reader will recognize both sides of the above expression as a linearized form of the Bernoulli equation [*Gill,* 1982, p. 276] for each baroclinic mode. Therefore this optimized boundary condition can be interpreted as a special linearization of the Bernoulli equation for each baroclinic mode.

2.2.2. A simplified baroclinic boundary condition. To numerically implement (16)-(17) we have to determine the vertical structure $\psi_m(z)$. The separation of the horizontal and the vertical dependencies for varying depths on open boundaries is a rather complicated problem. If we define a new constraint F_t as the sum of the modal constraints, $F_t = \sum_{m=1}^{M} F_t^m$, we have

$$-\int_\Gamma \int_{-H}^{0} (P^* - P^{o*})(u_n^* - u_n^{o*})dzds = F_t \qquad (18)$$

This constraint represents the baroclinic component of the flux of energy due to the differences between the reference and model-predicted modified pressures and normal velocity components. If this constraint is used in conjunction with the original baroclinic minimization problem (15), then the solution has the form

$$u_n^* = u_n^{o*} + \frac{1}{\lambda_t}\frac{(P^* - P^{o*})}{\rho_0} \tag{19}$$

$$\frac{1}{\lambda_t} = -\frac{F_t}{\int_\Gamma \int_{-H}^0 \frac{(P^*-P^{o*})^2}{\rho_0} dz ds} \tag{20}$$

Again, the Lagrange multiplier λ_t has the dimension of velocity and represents some average over the group velocities for the baroclinic modes on the open boundaries. Thus (19)-(20) can be considered as an approximation of (16)-(17) and represents a special linearization of the Bernoulli equation for the baroclinic part of the velocity that does not require the determination of the individual baroclinic modes. In shallow coastal areas in which the first baroclinic mode plays a dominant role the value of λ_t will be close to the value of the group velocity for the first baroclinic mode.

2.2.3. Modal decomposition using empirical orthogonal functions (EOFs). As we mentioned before, one of the difficulties using normal mode decomposition is determining the vertical structure on an open boundary with varying bathymetry. To overcome this problem, EOFs can be used to represent the vertical structure of variables on an open boundary. In EOF analysis a set of data can be represented in the following form:

$$\varphi_i(t) = \sum_{m=1}^{M} \gamma_m(i)\beta_m(t) \tag{21}$$

where $\varphi_i(t)$ is a value of variable φ measured at point i and time t, M is a number of EOF modes, γ_m are orthogonal and normalized functions representing the spatial structure, and β are amplitudes (also orthogonal) representing the time component. We introduce the σ vertical coordinate system:

$$\sigma = (z - \eta)/(H + \eta) \tag{22}$$

In a σ coordinate system the same number of vertical layers is maintained for each grid point in the horizontal direction. This allows us to draw an analogy between time in (21) and sigma levels. The expansion (equation (21)) separates the dependence of position and time. We also need to separate the horizontal structure from the vertical. By replacing time with sigma in an EOF analysis we can create the desired result of using EOFs to separate the vertical structure from the horizontal structure. P^* can be represented for each time step as

$$P^* = \sum_{m=1}^{M} h_m(\sigma)\beta_m(x,y) \tag{23}$$

where $h_m(\sigma)$ are orthogonal EOF modes representing the vertical structure and β represents the horizontal structure. The energy flux constraints are

$$E_t^m = -\int_\Gamma [\int_{-1}^{0} (u_n^* - u_n^{o*})h_m(\sigma)d\sigma] \bullet H(s)[\beta_m(s,t) - \beta_m^o(s,t)]ds \tag{24}$$

Energy flux E_t^m represents the contribution of mth EOF mode to the energy flux on the open boundary resulting from the differences between model and referenced values of velocities and modified pressure. Using these constraints with the original baroclinic minimization problem, (15) the following solution can be obtained:

$$u_n^* = u_n^{o*} + \sum_{m=1}^{M} \frac{1}{\lambda_t^m}\frac{h_m(\sigma)}{\rho_0}[\beta_m(s,t) - \beta_m^o(s,t)] \tag{25}$$

$$\frac{1}{\lambda_t^m} = -E_t^m/[\int_{-1}^{0} \frac{1}{\rho_0} h_m^2(\sigma)d\sigma \bullet \int_\Gamma H(s)[\beta_m(s,t) - \beta_m^o(s,t)]^2 ds] \tag{26}$$

3. Some Other Considerations

In terms of baroclinic boundary conditions, either (19)-(20) or (25)-(26) can be easily applied in the case where the open boundary crosses the location of the velocity. If the open boundary crosses the location of temperature or salinity (at the center of the grid cell), we can consider a baroclinic optimization problem similar to barotropic problems (3)-(8) or (9)-(10). However, in the baroclinic case the use of a condition like (19) rewritten with P^* as the unknown would be problematic. This is because of the nonlinear dependence of P^* on temperature and salinity. Instead of using (19), suppose we consider a linear approximation of the density on the open boundary:

$$\rho = \rho_r(-c_T T + c_S S)$$

where T and S are temperature and salinity, c_T is the thermal expansion of the water, and c_S is the salinity contraction. Let T^o be the reference values of temperature on the open boundary. Open boundary values for temperature can be determined from the following optimization problem:

$$\min_T J_T = \frac{g^2}{2}\int_\Gamma \int_{-H}^{0} \frac{{\rho_r}^2 {c_T}^2}{{N_{\rho_0}}^2 \rho_0}(T - T^o)^2 dz ds \tag{27}$$

$$c_0 \int_\Gamma \int_{-H}^{0} \rho_0 (T - T^o)(u_n^* - u_n^{o*})\, dz\, ds = T_f \tag{28}$$

where c_0 is the specific heat of the ocean water and N_{ρ_0} is the Brunt-Vaisala frequency for ρ_0 density [*Gill*, 1982]. T_f can be interpreted as the flux of internal energy through the open boundary, while J_T represents the potential energy due to the differences between the

T and T^o temperature distributions on the open boundary. A similar problem can be formulated to determine open boundary conditions for salinity.

Finally, in implementing our optimization methods we note that the calculated energy fluxes (F_t) only represent estimates of their true values. Suppose δ_t is the error in the estimation of F_t, for example, for problem (15)-(18), then $F_t^e = F_t + \delta$, where F_t^e is a true, unknown value of energy flux.

Thus we have to provide a best fit to the estimates of the energy fluxes in our optimization problems. To do this, we employ the regularization method [*Shulman and Lewis,* 1995, 1996; *Parker,* 1994]. In this case the parameter of regularization γ is introduced, and the constrained optimization problem (15)-(18) is reduced to the following unconstrained optimization problem:

$$\min_{u_n^*} J_r = \{\frac{1}{2}[F_t + \int_\Gamma \int_{-H}^0 (P^* - P^{o*})(u_n^* - u_n^{o*})\, dz\, ds]^2 + \gamma \frac{1}{2} \int_\Gamma \int_{-H}^0 \rho_0 (u_n^* - u_n^{o*})^2\, dz\, ds\} \qquad (29)$$

The solution to (29) can be obtained by using the optimality condition $\delta J_r / \delta u_n^* = 0$. The solution of (29) is still equation (19):

$$u_n^* = u_n^{o*} + \frac{1}{\lambda_t} \frac{(P^* - P^{o*})}{\rho_0} \qquad (30)$$

but with

$$\frac{1}{\lambda_t} = -\frac{F_t}{\int_\Gamma \int_{-H}^0 \frac{(P^* - P^{o*})^2}{\rho_0} dz ds + \gamma} \qquad (31)$$

The value of the parameter γ depends on the value of δ_t. If we know the value of δ_t, the value of γ can be chosen by substituting (30)-(31) into the left side of (18) and solving for γ (when the left side of (18) is equal to $F_t + \delta_t$). In our case, there is a high level of uncertainty in determining the norm of the error (δ_t). For this reason we used the maximum of the entropy integral approach for determining γ. The details of this approach are provided in Appendix B.

4. Numerical Simulations

4.1. Coupling Fine and Coarse Resolution Models

Optimized open boundary conditions can be used in coupling limited area models (LAM) with coarser resolution, larger-domain models. This coupling can be achieved through the choice of reference values of boundary variables and through the estimates of energy fluxes (F_t) on the open boundaries of the LAM. Two schemes can be considered to couple the models. **In the first scheme**, reference values in the optimization problem are interpolated data from the coarse grid model, and the energy flux is estimated from the interior solution of the LAM. **In the second scheme**, reference values in the optimization problem are estimated from the governing physics of the LAM (for example, by employing a modified Orlanski condition [*Camerlengo and O'Brien,* 1980], and the energy flux is estimated from the coarse grid model.

In the first scheme the estimate of energy flux from the interior solution of the LAM can be obtained in many different ways. For example, energy flux can be estimated by moving one grid row inside from open boundary. Alternatively, energy fluxes can be calculated for n grid rows inside of the open boundary and then can be extrapolated to the open boundary.

The success of OBCs and coupling schemes depends on the ability of the models to resolve the internal modes with their grid resolutions as well as on the relative sizes of the models grid resolutions. This is illustrated in section 4.3 where the results of testing and comparison of the coupling schemes are presented.

4.2. Model

The model used in this study is a version of the *Blumberg and Mellor* [1987] three-dimensional circulation model. This model is a primitive equation, free surface model. It uses the turbulence closure submodel developed by *Mellor and Yamada* [1982]. Horizontal mixing processes are introduced in order to parameterize subgrid scale processes and to damp small-scale computational noise. Horizontal viscosity and diffusivity are introduced in the momentum equations and in conservation equations for temperature and salinity. The *Smagorinsky* [1963] formula for horizontal mixing is used in which the horizontal diffusivity coefficients depend on the grid size and velocity gradients:

$$A_H = C dx dy [U_x{}^2 + V_y{}^2 + (U_y + V_x)^2/2]^{1/2}$$

where A_H is the coefficient of horizontal diffusivity, dx and dy are grid sizes in x and y directions, U and V are horizontal velocity components, subscripts x and y denote partial differentiations, and C is a constant taken to be 0.1.

The model uses a curvilinear, orthogonal grid in the horizontal and a bottom-following σ coordinate grid in the vertical. A mode-splitting technique is used in the model to separate fast moving external gravity waves and slow moving internal gravity waves. In this case the separation of the vertically integrated governing equations (barotropic, external mode) and the equations governing vertical structure (baroclinic, internal mode) is introduced. Boundary conditions are formulated for the barotropic and baroclinic modes separately and then adjusted to take into account the different truncation errors for those modes [*Blumberg and Mellor,* 1987]. For additional information on the model the reader is referred to *Blumberg and Mellor* [1987].

4.3. Simulations Over an Idealized Shelf/Slope

In this section our primary goal is the testing of baroclinic optimized open boundary conditions.

4.3.1. Test case 1. Simulations were conducted for the idealized shelf/slope shown on Figure 1 (top).

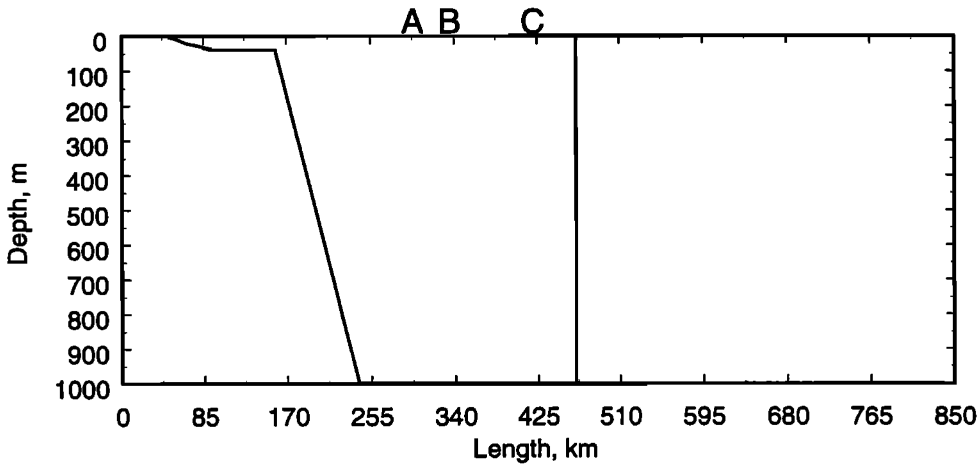

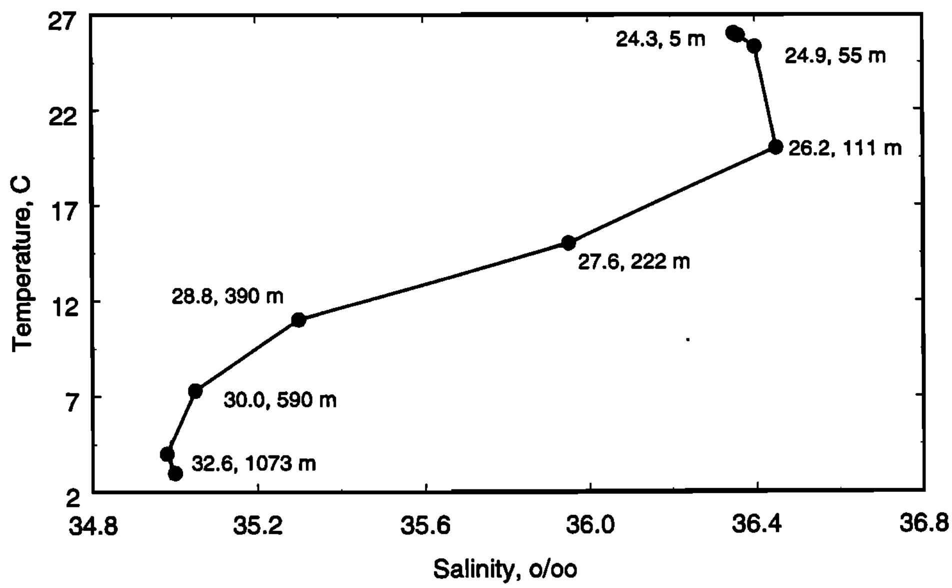

Figure 1. (top) Model domain for test case 1 with the location of the sections. (bottom) Temperature-salinity structure used for the model simulations. Numbers beside each point on bottom plot are σ_t and depth.

The offshore extent of the model area is 837.5 km. The longshore extent consists of three grid points (the first and third points are land). Therefore we have a channelized flow with motion only in the vertical and onshore/offshore directions. Two models were set up for this bathymetry. The first was a finer resolution model with an 8.375 km horizontal resolution (100 grid points) and 21 levels equally spaced in the vertical. The second was a coarser-grid model with a 25.125 km resolution and with only 10 evenly spaced levels.

Both these first two models were run by beginning at rest with only vertical variations of temperature and salinity (Figure 1, bottom). A bottom roughness of 3 mm was used in the bottom boundary layer formulation, and a minimum frictional coefficient of $2.5\text{x}10^{-3}$ was specified. On the open boundary (100th grid point) we forced these models with a surface height oscillation with an amplitude 1 m at the M_2 tidal frequency. The finer-grid model is used to provide us with "truth" velocities at three locations in the channel (A, B, and C in Figure 1, top). They are plotted in Figure 2 in terms of the total velocity minus the barotropic velocity for layers at depths of 5, 77, 183, 590, 800, and 930 m. At the beginning of the simulation the flow is barotropic. Baroclinic modes are eventually generated, first along the shelf slope and then propagating offshore. These baroclinic velocities are those we wish to reproduce in subsequent simulations.

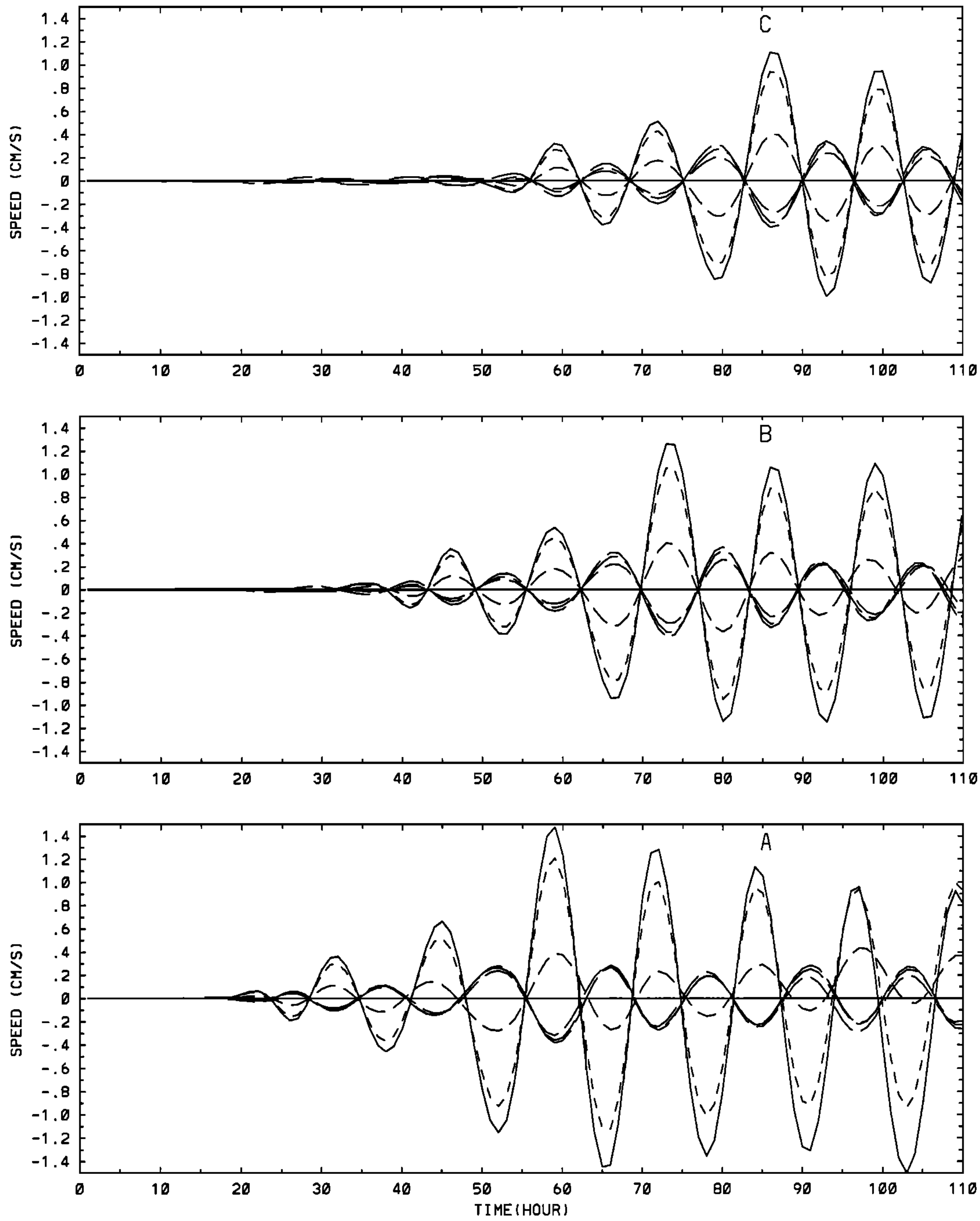

Figure 2. Test case 1 total velocity minus barotropic velocity for six layers (5, 77, 183, 590, 800, and 930 m deep) at three sections in the domain (the letter in the right corner of each plot corresponds to the section location on Figure 1).

The coarser-grid model is used to provide us with reference information for our optimized open boundary schemes. We ran the coarser grid model and saved time history information on sea surface elevation, barotropic and total velocity, temperature, and salinity. This information was interpolated to the location of the 55th grid cell of the finer-grid model, and it is these values that were used as reference values for open boundary conditions for a third model. The third model is a LAM that consists of only 55 grid cells of the original finer-grid model. It has the same horizontal and vertical resolution as the larger fine-grid model. This LAM is forced in the barotropic mode by using the reference sea level and vertically averaged velocity from the coarser-grid simulation in equation (6) but with $\lambda_t^0 = 1$ (i.e., the original *Flather* [1976] boundary condition). Coupling in the baroclinic mode is performed by using the two coupling schemes described in section 4.1.

In the framework of each coupling scheme we test the simplified baroclinic open boundary condition (19)-

(20), a decomposition of variables into orthogonal normal modes (16)-(17), and the use of EOF modes (25)-(26) instead of normal modes. To compare the results, the following relative model skill in prediction of velocity is used:

$$\zeta = [\sum_{t=1}^{T}\sum_{i=1}^{6}(\frac{u_i^{\text{LAM}} - u_i^{\text{OBS}}}{A_i^{\text{OBS}}})^2]^{1/2}$$

where u_i^{LAM} is the velocity from the LAM for layer i, u_i^{OBS} is the velocity from the first model (larger domain, finer grid) for layer i, and A_i^{OBS} is the maximum value of the baroclinic part of the first model velocity for layer i. Therefore the estimate ζ represents the relative error of the LAM simulation in comparison to the extended area run with the same resolution. The results of the application of the two coupling schemes are shown in Plate 1 (function ζ versus time).

The best results are given by the use of a simplified baroclinic boundary condition for scheme 2 (Plate 1, curve E). This has the following physical explanation. In this problem the internal gravity waves are moving in an offshore direction toward the open boundary of the LAM. The wavelength of the first baroclinic mode estimated from the normal mode analysis is $\sim$ 95.5 km. The LAM model (8.375 km grid size and 21 vertical levels) has enough resolution to resolve this mode, while the coarse-grid model (25.125 km grid size and 10 vertical levels) does not. Thus we would expect a better performance from coupling schemes that use a smaller amount of information from the coarse grid. Since reference values are taken from the coarse model in scheme 1, while scheme 2 uses only an energy flux estimated from the coarse model, scheme 2 results in a superior performance in comparison to scheme 1. For this reason the simplified baroclinic boundary condition for scheme 2 (Plate 1, curve E) has the best performance for this test. The use of additional (and more erroneous) information from the coarse grid as estimates of energy fluxes for the normal modes or for EOF (Plate 1, curves G and F) increases the error of prediction in comparison to the simplified open boundary condition for this scheme. At the same time, in scheme 1 the use of additional accurate information estimated from the fine-grid LAM model, as energy fluxes for normal modes or for EOF (Plate 1, curves C and D), decreases the error of prediction in comparison to the simplified open boundary condition for this scheme, which uses only the total baroclinic energy flux.

4.3.2. Test case 2. In this test case the performance of optimized open boundary conditions and coupling schemes is tested for the situation in which internal waves are moving in offshore and onshore directions. A bell-shaped sea mountain that is $\sim$ 75 km long and 300 m high was introduced in the extended area outside the open boundary of the LAM domain (see Plate 2, top). As in test case 1, two extended area models were set up for this bathymetry: a fine-resolution model with the same resolution as in test case 1 and a twice-coarser resolution model with grid spacing equal to 16.750 km. In this case both grids have enough resolution to resolve the first baroclinic mode. All other parameters remain the same as in test case 1.

As in previous experiments, both models were forced on the open boundary with the surface height oscillation with an amplitude 1 m at the M_2 tidal frequency.

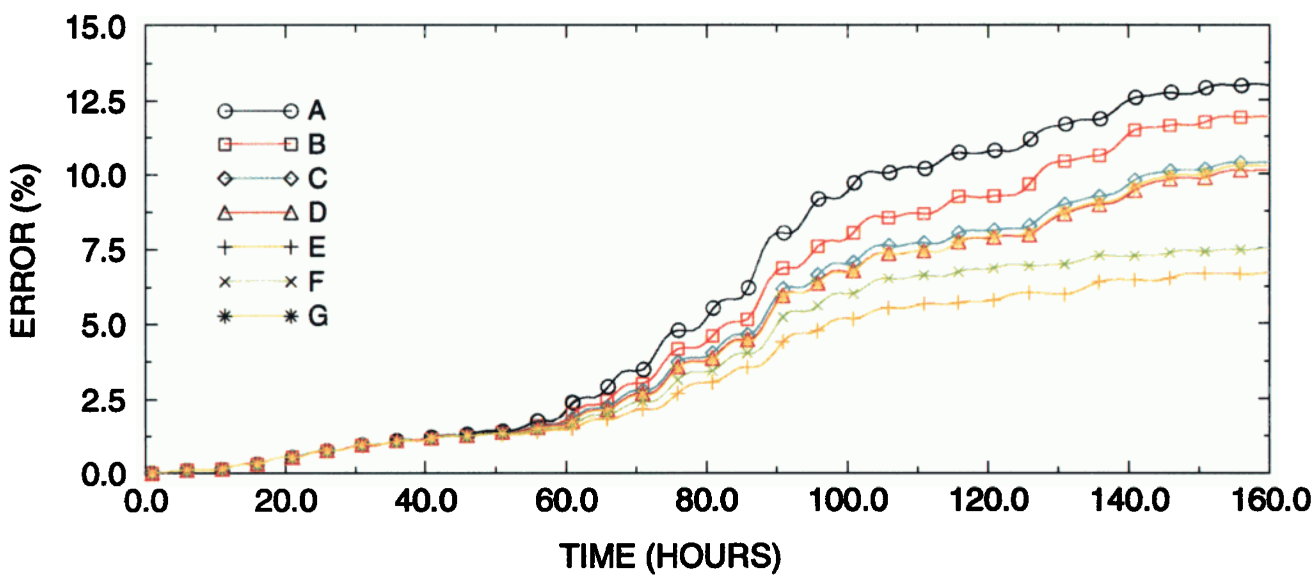

Plate 1. Test case 1 coupling of coarse- and fine-resolution models with the use of optimized open boundary conditions (error of prediction versus time): A, values for the open boundary of the fine-grid are equal to interpolated values from the coarse-grid model; B, scheme 1 of coupling without a modal decomposition; C, scheme 1 with the use of five EOF modes; D, scheme 1 with the use of five normal modes; E, scheme 2 of coupling without a modal decomposition; F, scheme 2 with the use of five EOF modes; and G, scheme 2 with the use of five normal modes.

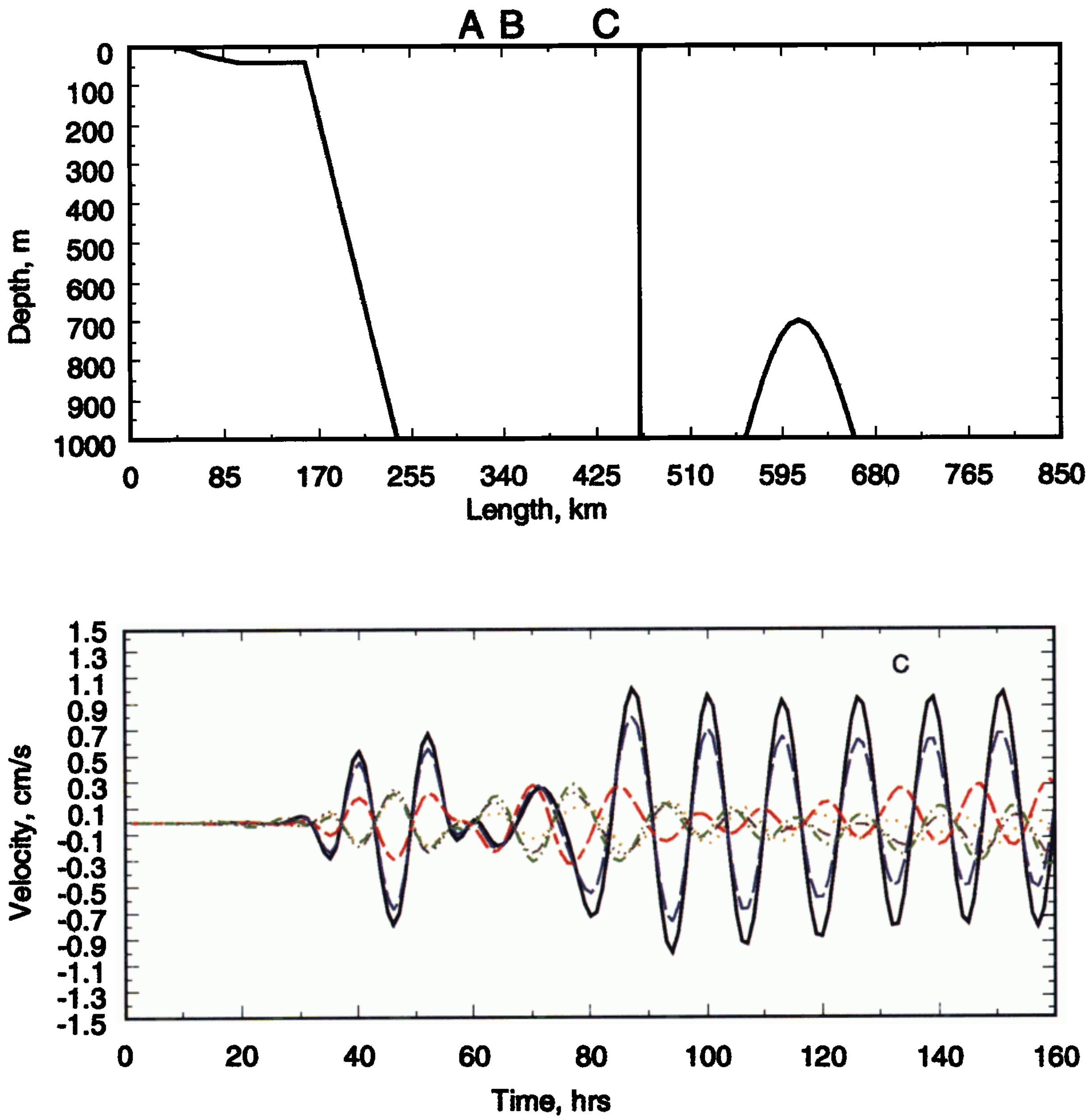

Plate 2. (top) Model domain for test case 2 with the location of the sections. (bottom) Total velocity minus barotropic velocity for six layers at station C.

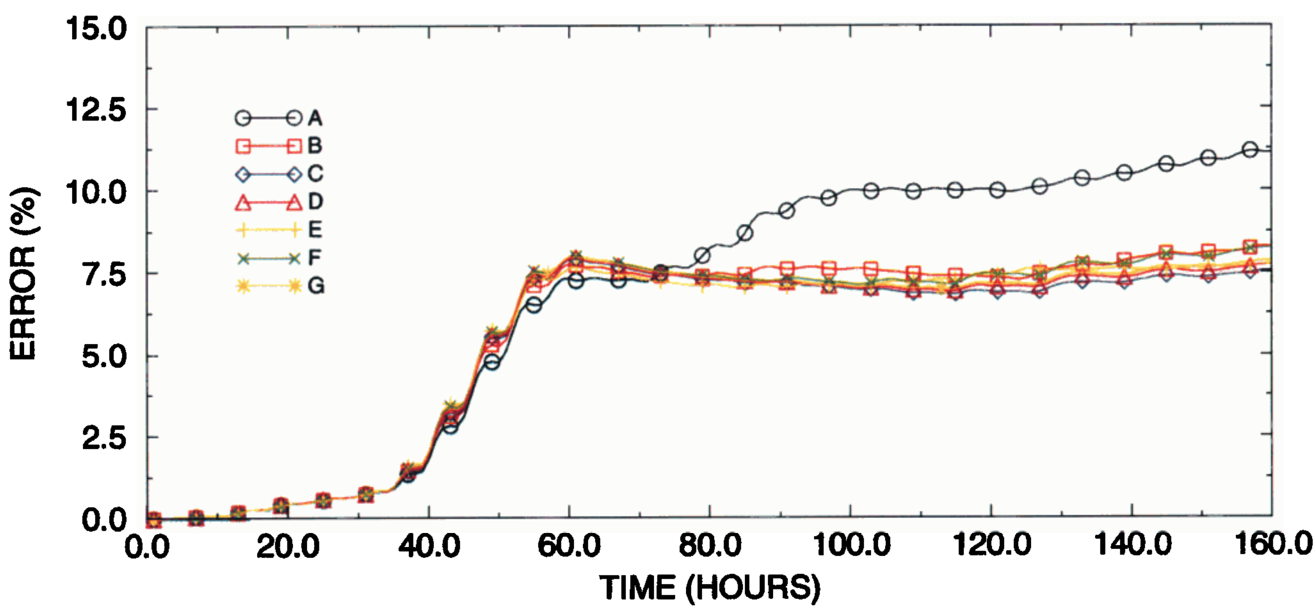

Plate 3. Same as plate 1 but for test case 2.

The total velocity minus the barotropic velocity for six layers are shown on Plate 2 (bottom) for station C. Comparison with the test case 1 (Figure. 2, top panel) shows a new baroclinic signal between 30 and 50 hours from the beginning simulations. This is internal wave moving in an onshore direction as a result of the interaction of the barotropic tide with the bathymetry of the sea mountain. As in test case 1, the sea surface elevation, barotropic and total velocities, and temperature and salinity data from the coarse-grid model were saved and interpolated to the open boundary of the LAM. In the framework of each coupling scheme we tested the simplified baroclinic open boundary condition (19)-(20), a decomposition of variables into orthogonal normal modes (16)-(17), and the use of EOF modes (25)-(26) instead of normal modes. The results are shown in Plate 3 (function ζ versus time). At the end of the simulations all coupling schemes with the use of the optimized open boundary conditions performed better than the nonoptimized condition, as in test case 1. However, there is little difference in the results between the use of coupling schemes 1 and 2. Also, the use of EOF or normal modes did not result in significant improvements in comparison to the simplified versions of these schemes. The reasons for this are as follows. The duration of simulations (160 hours) was chosen in order to avoid spurious reflections of baroclinic waves (first mode) from the open boundary of the extended area (it takes more than 160 hours for the first baroclinic mode to reach the open boundary of the extended area domain and come back to the open boundary of the LAM). In this case the extended fine-resolution model run provides a good estimate of the "exact" solution for comparisons with the results of coupling schemes. On the other hand it means that in both test cases the first baroclinic mode is the most dominant one. Therefore the addition of more normal or EOF modes does not give improvements in comparison to the simplified version of the optimized boundary condition that represents, as we show in appendix A, the averaging over the baroclinic modes. Also, in test case 2, both fine and coarse grids have enough resolution to resolve the horizontal variations of the first baroclinic mode. For this reason the results of simulations do not show significant differences between the application of schemes 1 or 2. Overall, the results of coupling the fine-resolution LAM with the coarse-grid model show that the above mentioned two optimized schemes for coupling models perform superior to one in which values on the open boundary of the LAM are simply equal to the interpolated ones from the coarse-grid model run.

5. Discussion and Conclusions

Methods have been developed for specifying barotropic and baroclinic open boundary conditions for regional ocean models. The methodologies provide for an optimized determination of variables at the open boundaries based on any reference boundary information (from observations, other model simulations, etc.) constrained by the physics of the flux of energy at the open boundary. Minimization techniques using Lagrange multipliers are applied to develop formulations that drive variables along open boundaries in regional models toward reference boundary information. The results are constrained to be consistent with the flux of energy at the open boundary so that the solution from the interior domain of the model influences the values of variables along the open boundaries. Minimization formulations have been developed in the linearized forms of the Bernoulli equations for the barotropic as well as the baroclinic modes and do not require the a priori specification of spatial or temporal scales or the estimation of phase speeds. Moreover, it is shown that the time averages of the Lagrange multipliers represent the group velocities for the baroclinic modes in the case of the adjustment under gravity of the continuously stratified incompressible fluid.

Optimization problems are solved by using the regularization approach in order to take into account the errors of the data being assimilated. At the same time, because of the difficulty of specifying reliable estimates of data errors on the open boundary, the approach that makes the fewest unnecessary assumptions about errors (the method of maximum of entropy integral) was used for choosing the regularization parameter. The future development of reliable models of errors on the open boundary and in its vicinity might improve the application of the regularization approach and improve the performance of optimized open boundary conditions.

Derived open boundary conditions can be interpreted as some special flow relaxation schemes [*Davies,* 1976; *Martinsen and Engedahl,* 1987], where boundary values are relaxed toward the reference boundary values. The conditions have coefficients of relaxation, Lagrangian multipliers (λ_t), which change over time and provide the adaptation of the boundary values to the change in the energy flux through the open boundary.

The optimized open boundary conditions result in a significant reduction of errors when compared to the commonly used nonoptimized schemes. The results of the barotropic simulations and sensitivity tests [*Shulman and Lewis,* 1995; *Shulman,* 1997] showed that the application of optimized versions of radiation open boundary conditions reduce significantly the error of model predictions compared to the use of nonoptimized radiation conditions. Radiation-type open boundary conditions transmit the level of errors in the reference values into the interior model domain, while the optimized versions of these conditions correct the energy input from the reference values and thus result in a reduction in errors.

The proposed technology for coupling a fine-resolution, limited area model (LAM) with a coarse-resolution basin-scale model is based on optimized open boundary conditions. Two schemes are used to couple the models. In the first scheme, reference values in the optimization problem are interpolated results from the coarse-grid model, and the energy flux is estimated from interior solution of the LAM. In the second scheme, reference values in the optimization problem are estimated from the governing physics of the LAM (for example, by employing a modified Orlanski condition [*Camerlengo and O'Brien*, 1980]), and the energy flux is estimated from the coarser-grid model.

The proposed technology was tested for the case of idealized shelf and shelf slope. In the framework of each coupling scheme we tested the simplified baroclinic open boundary condition, a decomposition of variables into orthogonal normal modes, and the use of EOF modes instead of normal modes. In test case 1 the generated baroclinic waves are moving in the offshore direction toward the open boundary of the LAM domain. The test was constructed in such a way that the coarse-grid model does not have enough resolution to resolve these baroclinic modes. The results of coupling a fine-resolution LAM with a coarse-grid model show that the optimized schemes for coupling models perform better when compared to those in which values on the open boundary of a LAM are simply equal to the interpolated values from the coarse-grid model run. Since the reference values are taken from the coarse model in scheme 1, while scheme 2 uses only an energy flux estimated from the coarse model, scheme 2 results in a superior performance in comparison to scheme 1 (see Plate 1). The use of additional erroneous information from the coarse grid as estimates of energy fluxes for the normal or EOF modes (Plate 1, curves G and F) increases the error of prediction in comparison to the simplified open boundary condition for the second scheme. In scheme 1 the use of additional accurate information estimated from the fine-grid LAM model as energy fluxes for the normal modes or for the EOF (Plate 1, curves C and D) decreases the error of prediction in comparison to the simplified open boundary condition for this scheme, which uses only the total baroclinic energy flux.

In test case 2 the performance of optimized open boundary conditions and coupling schemes was tested in the case when internal waves are moving in offshore and inshore directions. Also, both grids had enough resolution to resolve the first baroclinic mode. Because of this and the fact of the dominance of the first baroclinic mode, the results of simulations did not show significant differences between the applications of schemes 1 and 2. At the same time both schemes showed performances superior to that of the nonoptimized scheme. Overall, the results of coupling the fine-resolution LAM with the coarse-grid model show that the above mentioned two optimized schemes for coupling models perform superior to one in which values on the open boundary of the LAM are simply equal to the interpolated ones from the coarse-grid model run.

In the proposed coupling schemes the energy fluxes are estimated either from coarse- or fine-grid model results. In the future we would like to explore a way of combining model outputs with the oceanographic measurements in order to estimate energy fluxes used in optimized open boundary conditions.

Appendix A

Below we show the physical interpretation for Lagrange multipliers in optimized boundary conditions. It is known that the Lagrange multiplier of any constraint measures the rate of change in the objective function with respect to changes in that constraint function. According to (14)-(15) and (16)-(17) the Lagrange multiplier $1/\lambda_t^m$ measures the rate of change in the kinetic energy at the open boundary in relation to changes in the energy flux of the mth mode on the open boundary:

$$\frac{1}{\lambda_t^m} = \frac{\delta E^k}{\delta F_t^m}$$

where δ denotes a small perturbation in value and E^k is kinetic energy. If the modes are not coupled, we have

$$\frac{1}{\lambda_t^m} = \frac{\delta E_m^k}{\delta F_t^m} \tag{A1}$$

where E_m^k is the kinetic energy of the mth mode. For many waves the following relation is valid [*LeBlond and Mysak*, 1978]:

$$< \delta F_t^m >= C_g^m (< \delta E_m^k > + < \delta E_m^p >) \tag{A2}$$

where $< >$ is the average over the phase, C_g^m is the group velocity for the mth mode, and δE_m^p is the change in potential energy for the mth mode on open boundary. From (A1) we have:

$$< \delta F_t^m > \approx < \lambda_t^m >< \delta E_m^k > \tag{A3}$$

In our optimization problem, for each time step the perturbation in F_t^m can be caused only by a perturbation in velocity. Therefore we can suppose that $\delta E_m^p \approx 0$. In this case, from (A2) and (A3) it follows that

$$< \lambda_t^m > \approx C_g^m \tag{A4}$$

Also, the same conclusions can be drawn from the consideration of the adjustment under gravity of the continuously stratified incompressible fluid [*Gill*, 1982; *LeBlond and Mysak*, 1978]. Let p' be a small pressure perturbation from rest. For simplicity we will work with a modified pressure defined as

$$P = p + \rho_0 \psi \tag{A5}$$

also, we choose $P^o = \overline{P}$. In this case we have

$$\frac{(P^* - P^{o*})}{\rho_0} = \frac{(p - p^o)}{\rho_0} = \frac{p'}{\rho_0} \tag{A6}$$

where p' is a small pressure perturbation from rest, which can be represented in normal modes as

$$p' = \sum_{m=1}^{M} \psi_m(z) \varphi_m(x, y, t) \tag{A7}$$

Consider horizontally propagating waves of the form

$$\varphi_m = A_m \exp(iS_m) \tag{A8}$$

where A_m is a constant and $S_m = k_1^m x + k_2^m y - \omega_m t$. We have the following dispersion relation [*LeBlond and Mysak,* 1978]:

$$\omega^2 = \omega_m^2 = g h_m^e K_m^2 + f^2 \qquad m = 1, M \tag{A9}$$

where h_m^e is the equivalent depth for the mth mode, $K_m^2 = (k_1^m)^2 + (k_2^m)^2$, and f is the Coriolis parameter. The horizontal velocity components for this problem have the form [*LeBlond and Mysak,* 1978, pp. 142-143]

$$u_m = \frac{\omega_m k_1^m + i f k_2^m}{\rho_0(\omega_m^2 - f^2)} \psi_m(z) A_m \exp(iS_m) \tag{A10}$$

$$v_m = \frac{\omega_m k_2^m + i f k_1^m}{\rho_0(\omega_m^2 - f^2)} \psi_m(z) A_m \exp(iS_m) \tag{A11}$$

where u^m and v^m are horizontal velocity components for mth normal mode. Therefore the normal component of the velocity on the open boundary has the following expression:

$$\begin{aligned} u_{m,n} &= \frac{1}{\rho_0(\omega_m^2 - f^2)}[(\omega_m k_1^m + i f k_2^m)\cos(n,x) \\ &\quad + (\omega_m k_2^m + i f k_1^m)\cos(n,y)] \\ &\quad \bullet \psi_m(z) A_m \exp(iS_m) \end{aligned} \tag{A12}$$

where $u_{m,n}$ is the normal component velocity for the mth mode on the open boundary and $\cos(n,x)$ and $\cos(n,y)$ are cosines between the normal to the open boundary and the x and y axes. Now we estimate F_t^m (suppose, for simplicity, that $u_n^{o*} = 0$). By substituting (A12) into (14) and taking into account (13), we have the following expression for F_t^m:

$$\begin{aligned} F_t^m &= -\frac{1}{(\omega_m^2 - f^2)}[(\omega_m k_1^m + i f k_2^m)\cos(n,x) \\ &\quad + (\omega_m k_2^m + i f k_1^m)\cos(n,y)] \int_{-H}^{0} \frac{1}{\rho_0}\psi_m^2(z)dz \\ &\quad \bullet \int_\Gamma A_m^2 \exp(i2S_m) ds \end{aligned} \tag{A13}$$

and from (17) we have:

$$\begin{aligned} \frac{1}{\lambda_t^m} &= \frac{1}{(\omega_m^2 - f^2)}[(\omega_m k_1^m + i f k_2^m)\cos(n,x) \\ &\quad + (\omega_m k_2^m + i f k_1^m)\cos(n,y)] \end{aligned} \tag{A14}$$

According to our boundary condition (16), we have

$$\begin{aligned} u_{m,n} &= \frac{1}{\lambda_t^m}\frac{\psi_m(z)}{\rho_0}\varphi_m(s,t) \\ &= \frac{1}{\lambda_t^m}\frac{\psi_m(z)}{\rho_0} A_m \exp(iS_m) \end{aligned} \tag{A15}$$

If we substitute (A14) into (A15), we will get expression (A12); therefore the open boundary condition (16)-(17) provides the correct continuation of the domain velocity to the open boundary. Suppose that $k_2^m = 0$ and that the open boundary is parallel to the y axis. In this case we have

$$\frac{1}{\lambda_t^m} = \frac{\sqrt{g h_m^e + \frac{f^2}{K_m^2}}}{g h_m^e} \tag{A16}$$

Therefore according to (A16) and *LeBlond and Mysak,* [1978] we have

$$\lambda_t^m = C_{mg} \tag{A17}$$

where C_{mg} is the group velocity.

Appendix B

Below we describe the approach for choosing the value of the regularization parameter γ for the optimization problem (29). We introduce the following notation:

$$\mu = \frac{\gamma}{\int_\Gamma \int_{-H}^{0} \frac{(P^* - P^{o*})^2}{\rho_0} dz ds} \tag{B1}$$

and we will discuss the value of the nondimensional parameter μ. Suppose that velocity $u_{n,ex}^*$ is a solution of the optimization problem when F_t and P^* are the exact values for the energy flux and pressure. We do not know the function $u_{n,ex}^*$, but we have the function $u_n^*(\mu)$ from (30) with the λ_t from (31). Some norm of the product $\mu \partial u_n^* / \partial \mu$ (corresponding to the first member of the Taylor series of the difference between $u_n^*(\mu)$ and $u_{n,ex}^*$) can be used to estimate the difference between $u_n^*(\mu)$ and $u_{n,ex}^*$ and to estimate the optimal value of μ and γ. Let us introduce the following norm:

$$\varphi^2 = \int_\Gamma \int_{-H}^{0} \rho_0 (\mu \frac{\partial u_n^*}{\partial \mu})^2 ds$$

According to (B1), (30) and (31) we have

$$\varphi^2 = \frac{{F_t}^2}{\int_\Gamma \int_{-H}^{0} \frac{(P^* - P^{o*})^2}{\rho_0} dz ds} \frac{\mu^2}{(1+\mu)^4} \tag{B2}$$

Let us introduce the normalized distribution function

$$f(\mu) = \frac{\varphi^2(\mu)}{\int_0^\infty \varphi^2(\mu) d\mu}$$

which is, according to (B2), equal to

$$f(\mu) = 3\frac{\mu^2}{(1+\mu)^4}$$

We choose the value for μ according to the maximum entropy method:

$$\max_\mu [-f(\mu) \ln f(\mu)] \tag{B3}$$

In this case by maximizing entropy over all values of μ, we are picking a μ that makes the fewest unnecessary assumptions (most cautious hypothesis). The solution for (B3) is

$$\mu = 1 \tag{B4}$$

$$\gamma = \int_\Gamma \int_{-H}^{0} \frac{(P^* - P^{o*})^2}{\rho_0} dz ds \tag{B5}$$

Acknowledgments. This work was supported by the Office of Naval Research (the Naval Ocean Modeling and Prediction program). The authors wish to thank A. F. Blumberg for many helpful discussions and J. J. O'Brien for stimulating comments. We would like to thank D. Fox and P. Martin of Naval Research Laboratory for the program code of EOF and normal mode decomposition. Also, we would like to thank the anonymous reviewers for many helpful comments. This work was supported in part by grants of HPC time from the DoD HPC Centers at U. S. Naval Oceanographic Office, Stennis Space Center, Mississippi and U.S. Army Corps of Engineers Waterways Experiment Station (CEWES).

References

Batchelor, G.K., *An Introduction To Fluid Dynamics*, 615 pp., Cambridge Univ. Press, New York, 1967.

Bennett, A. F., *Inverse Methods in Physical Oceanography*, 346 pp., Cambridge Univ. Press, New York, 1992.

Bennett, A. F., and P.C. McIntosh, Open ocean modeling as an inverse problem, *J. Phys. Oceanogr.*, 12, 1004-1018, 1982.

Blumberg, A., and L. Kantha, Open boundary condition for circulation models. *J. Hydraul. Eng.*, *111*, 237-255, 1985.

Blumberg, A., and G. L. Mellor, A description of a three-dimensional coastal ocean circulation model, in *Three Dimensional Coastal Models, Coastal Estuarine Sci*, Vol 4, edited by N.S. Heaps, pp. 1-16, AGU, Washington, D.C., 1987.

Bogden, P.S., P. Malanotte-Rizolli, and R. Signell, Open-ocean boundary conditions from interior data: Local and remote forcing of Massachusetts Bay, *J. Geophys. Res.*, 101, 6487-6500, 1996.

Camerlengo, A. L., and J. J. O'Brien, Open boundary conditions in rotating fluids, *J. Comput. Phys.*, *35*, 12-35, 1980.

Chapman, D., Numerical treatment of cross-shelf open boundaries in a barotropic coastal ocean model, *J. Phys. Oceanogr.*, *15*, 1060-1075, 1985.

Davies, H. C., A lateral boundary formulation for multi-level prediction models, *Q. J. R. Meteorol. Soc.*, *102*, 405-418, 1976.

Flather, R. A., A tidal model of the northwest European continental shelf. *Mem. Soc. R. Sci. Liege* , Ser. 6, 10, 141-164, 1976.

Fletcher, R., *Practical Methods Of Optimization.*, 436 pp., John Wiley, New York, 1987.

Gill, A. E., *Atmosphere-Ocean Dynamics*, 662 pp., Academic, San Diego, Calif., 1982.

Gunson, J. R., and P. Malanotte-Rizzoli, Assimilation studies of open-ocean flows, 1, Estimation of initial and boundary conditions. *J. Geophys. Res.*, *101*, 28,457-28,472, 1996a.

Gunson, J. R., and P. Malanotte-Rizzoli, Assimilation studies of open-ocean flows, 2, Error measures with strongly nonlinear dynamics. *J. Geophys. Res.*, *101*, 28,473-28,488, 1996b.

Hellerman, S. and M. Rosenstein, Normal monthly wind stress over the world ocean with error estimates. *J. Phys. Oceanogr.*, *13*, 1093-1104, 1983.

Jensen, T.G., Equatorial variability and resonance in a wind-driven Indian Ocean model, *J. Geophys. Res.*, *98*, 22,533-22,552, 1993.

LeBlond, P.H., and L. A. Mysak, *Waves in the Ocean*, 602 pp., Elsevier, New York, 1978.

Martinsen, E. A., and H. Engedahl, Implementation and testing of a lateral boundary scheme as an open boundary condition in a barotropic ocean model, *Coastal Eng.*, *11*, 603-627, 1987.

Mellor, G. L., and T. Yamada, A hierarchy of turbulence closure models for planetary boundary layers, *J. Atmos. Sci.*, 31, 1791-1896, 1982.

Oliger, J., and A. Sundstrom, Theoretical and practical aspects of some initial boundary value problems in fluid dynamics, *SIAM J. Appl. Math.*, *35*,419-446, 1978.

Orlanski, I., A simple boundary condition for unbounded hyperbolic flows. *J. Comput. Phys.*, *21*, 251-269, 1976.

Parker, R. L., *Geophysical Inverse Theory*, 386 pp., Princeton Univ. Press, Princeton, N.J., 1994.

Reid, R. O., and B. R. Bodine, Numerical model for storm surges in Galveston Bay, *J. Waterw. Harbors Coastal Eng. Div. Am. Soc. Civ. Eng.*, *94*, 33-57, 1968.

Seiler, U., Estimation of the open boundary conditions with the adjoint method, *J. Geophys. Res.*, *98*, 22,855-22,870, 1993.

Shulman, I., Local data assimilation in specification of open boundary conditions, *J. Atmos. Oceanic Technol.*, *14*, 1409-1419, 1997.

Shulman, I., and J. K. Lewis, Optimization approach to the treatment of open boundary conditions, *J. Phys. Oceanogr.*, *25*, 5, 1006-1011, 1995.

Shulman, I., and J. K. Lewis, Optimized boundary conditions for coastal modeling, in *Estuarine and Coastal Modeling*. edited by M. L. Spaulding and R. T. Cheng, pp. 268-282, American Society of Civil Engineers, New York, 1996.

Smagorinsky, J., General circulation experiments with the primitive equations, I, The basic experiment, *Mon. Weather Rev.*, *91*, 99-164, 1963.

Zou, J., W.W. Hsieh, and I.M. Navon, Sequential open-boundary control by data assimilation in limited-area model, *Mon. Weather Rev.*, *123*, 2899-2909, 1995.

Zou, X., I. M. Navon, M. Berger, P. K. Phua, T. Schlick, and F. X. LeDimet, Numerical experience with limited memory quasi-Newton methods for large-scale unconstrained nonlinear minimization, *SIAM J. Control Optim.*, *3*, 582-608, 1993.

J. K. Lewis, Scientific Solutions, Inc., 4875 Kikala Road, Kalaheo, HI 96741. (e-mail: ocnphys@aol.com)

J. G. Mayer, Department of Scientific Computing, University of Southern Mississippi, Hattiesburg, MS 39402. (e-mail: jgmayer@ocean.otr.usm.edu)

I. Shulman, Institute of Marine Sciences, University of Southern Mississippi, Bldg 1103, Room 249, Stennis Space Center, MS 39529. (e-mail: shulman@coam.usm.edu)

(Received October 15, 1997; revised November 18, 1998; accepted January 29, 1999.)